Helgol Mar Res (2001) 55:12–22
DOI 10.1007/s101520000064

ORIGINAL ARTICLE

Hendrik Schubert · Sigrid Sagert
Rodney Malcolm Forster

Evaluation of the different levels of variability in the underwater light field of a shallow estuary

Received: 15 September 1999 / Received in revised form: 7 April 2000 / Accepted: 17 April 2000 / Published online: 9 January 2001

Abstract The underwater light climate of a shallow estuary located at the southern coast of the Baltic Sea has been investigated, with special emphasis on the spectral irradiance composition and on short-term irradiance fluctuations caused by vertical mixing and wave focussing. The inherent optical properties of the water body were dominated by phytoplankton pigment absorption in the long-wavelength range and by coloured, dissolved organic matter (cDOM) absorption in the wavelength range <500 nm, including ultraviolet-A (UV-A) and ultraviolet-B radiation (UV-B). Pronounced particulate scattering combined with the absorption values to give very high attenuation coefficients, especially for the shorter wavelengths of UV-B radiation. Photosynthetically active radiation (PAR) was found to be reduced to 1% of the surface value within 0.8 m in the inner, hypertrophic end of the estuary and within 1.9 m in the outer, eutrophic parts of this system, with corresponding 1% penetration depths for UV-B of 0.13 and 0.31 m. During late winter and early spring, the period when reduced atmospheric ozone concentrations and enhanced UV-B have been reported over northern Europe, the irradiance levels in the water column were greatly reduced, due to strong attenuation by ice cover and overlying snow. cDOM concentration of the water was also found to remain at a high level during these periods, and indeed throughout the year, thus reducing the exposure of organisms to UV-R and PAR still further. A complex irradiance regime was found in this system, with irregular and high amplitude fluctuations caused by wind-induced vertical mixing and wave focussing being superimposed upon the solar-angle-dependent seasonal and daily cycles. The methods used to quantify the short-term fluctuations are described, and their relevance to phytoplankton physiology is discussed. The wave-focussing effect is unique to the aquatic environment, and measurements showed that average subsurface irradiances could be increased by up to 5 times for periods lasting for <1 s. The highest irradiances recorded during wave-focussing events reached over 9,000 µmol photons m^{-2} s^{-1}.

Keywords Ultraviolet radiation · Light climate · Dissolved organic matter · Wave focussing

Communicated by K. Lüning

H. Schubert (✉) · S. Sagert
Ernst-Moritz-Arndt-Universität Greifswald,
Institut für Ökologie/AG Pflanzenökologie,
Grimmer Strasse 88, 17487 Greifswald, Germany
e-mail: schubh@mail.uni-greifswald.de
Tel.: +49-3934-864123, Fax: +49-3834-864114

R.M. Forster
Nederlands Instituut voor Oecologisch Onderzoek,
Centrum voor Estuariene en Mariene Oecologie, NIOO-CEMO,
PO Box 140, 4400 AC Yerseke, The Netherlands

Introduction

Ecophysiological studies dealing with any kind of irradiance effects on organisms first require knowledge about the irradiance climate acting on the organisms to be studied. In the aquatic environment the underwater light climate exhibits a high degree of variability, both qualitatively (changes in spectral composition) as well as quantitatively. The frequencies of changes in spectral composition and absolute irradiance availability in natural environments range from years down to milliseconds. Long-term irradiance variations are caused by seasonal changes in the aspect of the earth to the sun, and midterm variations can be caused by, for example, changes in the quantity of absorbing and scattering materials in the water column.

Even though such variations, as well as the optical properties of the aquatic environment, have been very well studied (Jerlov 1951, 1976; Preisendorfer 1988; Kirk 1994), we know little about short-term (hours, minutes, seconds) irradiance variations caused for example by wave effects (Stramski and Legendre 1992; Wing et al. 1993; Wing and Patterson 1993) or by vertical mixing (Webster 1990; Webster and Hutchinson 1994; Hutchinson and Webster 1994).

During the past decade, however, interest in the ecophysiological effects of short-term irradiance fluctuations has increased. Several studies of the acclimation strategies of planktonic as well as benthic algae to short-term irradiance fluctuations have been published, most of them based on assumptions rather than field measurements of the magnitude and frequency of these fluctuations (Trenkensu et al. 1976; Kromkamp et al. 1992; Stramski et al. 1993; Tichy et al. 1995). As photosynthetic reactions and acclimation mechanisms react non-linearly to irradiance, and absorption of light by photosynthetically active pigments shows distinct spectral dependency (for reviews see: Falkowski and LaRoche 1991; Allen 1992; Barber and Andersson 1992; Franklin and Forster 1997), both qualitative and quantitative variations in the light field should be taken into account, particularly in the context of ultraviolet-B (UV-B) radiation effects and when studying the effects of supersaturating solar irradiances on autotrophic organisms.

In the following paper we present an overview of the natural variability existing in the underwater light climate of a series of shallow estuarine lagoons (or "boddens") located on the south-western coastline of the Baltic Sea, with special emphasis on the high-frequency irradiance fluctuations. This system, the locally named "Darss-Zingst Boddenkette" (DZBK) has a rather narrow connection to the open Baltic. This, together with the absence of tides in the Baltic, results in only limited water exchange between the estuary and the sea. Fluctuations in water level are driven mainly by differences in air pressure over the Baltic region. As a result, a salinity gradient (0–12 psu), combined with a gradient in eutrophication level (hyper-mesotrophic) can be observed in this system, which makes it an excellent study area for ecophysiological and biooptical investigations. A detailed description of the study area is given by Schiewer et al. (1993).

Material and methods

Irradiance measurements

Scalar underwater irradiance was measured with a high-resolution spectroradiometer (SR-9910; Macam Photometrics, Livingston, Scotland) equipped via a 10-m light guide with a spherical light collector of 0.7 cm diameter. Surface irradiance was measured with a cosine-corrected light collector. All optical components were constructed from high-grade quartz or teflon to enable measurements to be made at wavelengths of 250–800 nm. Successive underwater scans at depth intervals between 20 and 150 cm were used to calculate the diffuse attenuation coefficient, $K_{o(\lambda)}$ (Smith 1968). All spectral irradiance measurements are presented in quantametric units (µmol photons m^{-2} s^{-1}). Calibration of both absolute sensitivity and wavelength accuracy were made at regular intervals against voltage-stabilised deuterium and tungsten standard lamps (Macam SR-990) traceable to the National Physical Laboratory, London, UK.

Absorption

Total absorption of particulates plus dissolved organic materials (cDOM) [$a_{t(\lambda)}$], was measured in a 1-cm quartz cuvette placed in the absorption measurement accessory of a F4010 spectrofluorometer (Hitachi, Kyoto). The sample was scanned with both monochromators in synchronous mode, in order to suppress the strong autofluorescence which was noted in DZBK samples. Whilst not affecting measurements in the visible region of the spectrum, this artefact was particularly pronounced in the UV region when samples were scanned in a standard spectrophometer. Absorption of dissolved components [$a_{d(\lambda)}$], was determined by first filtering samples through glass fibre filters (GF-92; Schleicher and Schuell, Germany), then measuring the optical density of the filtrate between 300 and 750 nm against a reference of deionised water.

Absorption [$a_{(\lambda)}$, m^{-1}] was calculated from optical density [$OD_{(\lambda)}$] in the 1-cm cuvette using: $a_{(\lambda)}=OD_{(\lambda)}\times\ln(10)\times100$.

Particulate absorption [$a_{p(\lambda)}$] was calculated as: $a_{p(\lambda)}=a_{t(\lambda)}-a_{d(\lambda)}$. Values of absorption for pure water [$a_{w(\lambda)}$] were taken from Smith and Baker (1981).

Chlorophyll *a* concentration of the samples was determined after overnight extraction of the filters in *N*,*N*-dimethylformamide, and using the equations of Porra et al. (1989).

Short-term variations in incident irradiance

Vertical mixing was estimated by means of a fluorescent dye injected approximately 2–5 cm below the water surface. Circulation time was determined with a stopwatch, and windspeed by means of a field anemometer. The diameter of a circulation cell was determined by measuring the distance between the foam bands, representing the distance between two downwelling areas (i.e. the diameter of two cells). Wind speed and direction were monitored continuously with an anemometer located on a 10-m mast at the field station of the University of Rostock, Zingst.

Wave-focussing effects were measured with a custom-made instrument (Bornitz and Gagelmann 1995) which measured photosynthetically active radiation (PAR) underwater with a time-resolution of 28 µs. The instrument was kept at a fixed position, the 1-s measurement period was started manually and actual depth underneath water surface measured simultaneously by means of a ruler attached to the side of the sensor holder. Calibration and measurement procedures as well as hardware details are described also in Schubert (1996b).

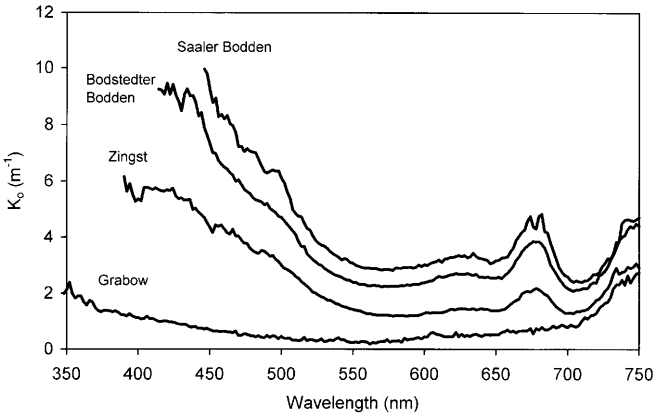

Fig. 1 Quasi-inherent optical properties of water bodies found along an east-west profile through the Darss-Zingst Boddenkette (DZBK). Attenuation spectra (K_o) were calculated from underwater measurements of scalar irradiance on 28 May and 29 May 1995 in the innermost, hypertrophic part of the estuary (Saaler Bodden), in the intermediate Bodstedter Bodden, at Zingst and in the Grabow, the outermost and mesotrophic seaward end of the estuary

Results

Attenuation and absorption

The attenuation spectra recorded along the DZBK (Fig. 1) show that, with the exception of the outermost

Table 1 Spectral composition of underwater irradiance in water types of different chlorophyll *a* concentration. The depth at which selected wavelengths are reduced to 1% of their surface value have been calculated from many different water bodies throughout the Darss-Zingst Bodden chain, and are also expressed as a percentage of the 1% depth for photosynthetically active radiation (*PAR*)

Chlorophyll *a* (mg m^{-3})	1% Depth (m)						
	300 nm	320 nm	360 nm	400 nm	570 nm	710 nm	PAR (400–700 nm)
0–20	0.28	0.88	1.44	2.42	10.0	4.18	6.24
20–50	0.19	0.31	0.42	0.59	2.30	2.09	1.93
50–80	0.09	0.17	0.33	0.46	2.00	2.00	1.57
80–120	0.10	0.15	0.25	0.36	1.64	1.92	1.38
120–250	0.10	0.13	0.2	0.27	0.96	1.24	0.84

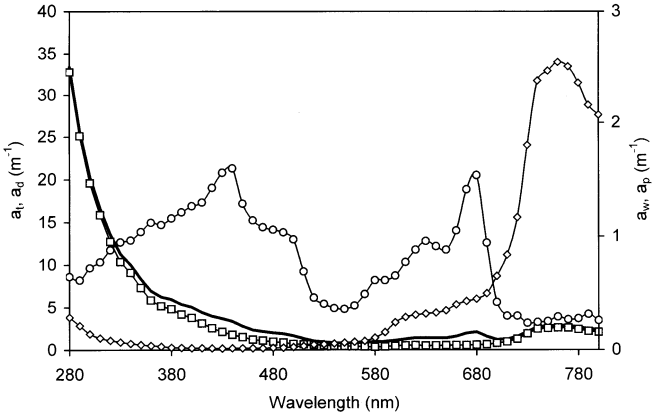

Fig. 2 Absorption spectra – analysis of the major absorbing components. Shown are the analysis of a water sample taken at Zingst on 25 July 1999 with a chlorophyll *a* content of 78 µg l^{-1}. Total absorption (a_t, *solid line*) and absorption of dissolved components (a_d, *open squares*) were measured in the absorption measurement equipment of a Hitachi F4010 spectrofluorometer. Particulate absorption (a_p, *open circles*) was calculated as the difference between a_t and a_d. Values for absorption of water (a_w, *open diamonds*) are taken from Smith and Baker (1981)

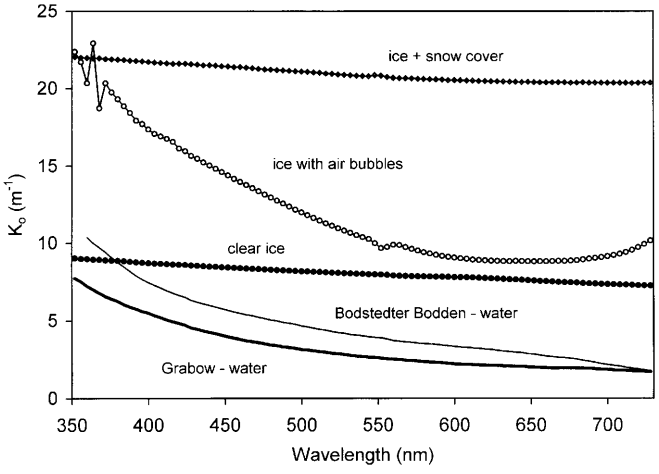

Fig. 3 Attenuation characteristics of different ice forms and water bodies underneath ice cover measured along the DZBK in January 1996

part of the bodden chain (Grabow), the system is very turbid. PAR was reduced to 1% of the surface value within 1.9 m, which is less than the average water depth of 2.0 m of the system (Table 1).

The attenuation spectra of the inner bodden waters showed distinct maxima at 620 and 675 nm, attributable to the absorption of phytoplankton pigments (phycocyanin and chlorophyll), as well as high values at wavelengths >730 nm which were due to attenuation by water itself.

Minima were observed in the green and the near-infrared wavelength range, indicating that these wavelengths penetrated deepest in the water column. For all except the outermost parts of the bodden chain, attenuation increased strongly with decreasing wavelength in the blue and especially in the UV wavelengths of the spectrum (Fig. 1). Table 1 shows that attenuation was clearly related to chlorophyll *a* content over the whole range of concentrations measured. However, at wavelengths <500 nm the strong increase in attenuation was more due to absorption by coloured, cDOM, the so called "Gelbstoffe" or "gilvins", already recognised by e.g. Piazena and Häder (1994). The effect of the different dissolved and suspended components in determining the overall absorption of the sample can be assessed by plotting their individual spectra (Fig. 2). The particulate absorption spectra, consisting mainly of phytoplankton pigments, accounts for approximately 70% of the total absorption in the wavelength interval 600–700 nm. Absorption of cDOM accounts for 50% of the total absorption at 500 nm, increasing to >80% of total absorption at wavelengths <450 nm, thus masking the signature of phytoplankton pigments in the blue region of the spectrum. The long-wavelength part of the spectra, e.g. >690 nm, was dominated almost exclusively by the absorption of water.

The absorption spectra in Fig. 2 were recorded in a way which reduced scattering effects (see Materials and methods), but the attenuation spectra shown in Fig. 1 are influenced in addition by particle scattering, which increases the pathlength of the incident light especially in the short-wavelength range. Therefore, attenuation at any given wavelength is always considerably higher than the corresponding absorption of the sample, and the difference becomes more noticeable at shorter wavelengths.

Due to the high concentration of cDOM in the DZBK (concentrations are typically >10 mg C l^{-1} for the inner

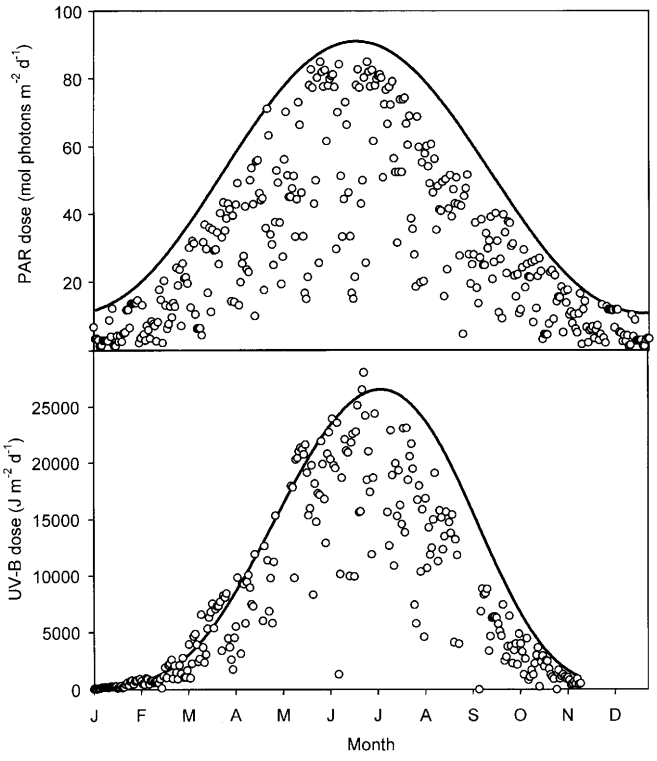

Fig. 4 *Upper panel*, comparison between theoretical maximum and measured daily irradiance doses (photosynthetically active radiation, *PAR*) at Zingst in 1997. Calculation of maximum daily dose (*solid line*) was performed by means of the spreadsheets published by Walsby (1997). PAR was calculated from global radiation data logged by a sensor on the roof of the University of Rostock field station at Zingst. *Lower panel*, comparison between theoretical maximum and measured daily ultraviolet-B (*UV-B*) doses at Zingst in 1998. Calculation of maximum daily dose (*solid line*) in the wavelength interval 290–314 nm was done by means of the computer model of Björn and Murphy (1985). UV-B was continuously logged with an Eldonet sensor located also at the field station

areas of the estuary), absorption in the UV region of the spectrum is extremely high (Fig. 2). Absorption, and attenuation coefficients increase exponentially as wavelength decreases <400 nm. This results in 1% depths for UV-B of <20 cm throughout most of the bodden system as well as 1% depths <30 cm for the exchange water at the mouth of the estuary and in the adjacent areas of the Baltic Sea (Table 1). The high cDOM content of the bodden waters is a product mainly of the catchment area of the system, which consists in many places of low-lying fens and mires.

A special case with regard to underwater irradiance, which has not been shown in the measurements presented so far, occurs during periods of ice cover. Ice coverage of all, or parts of the Baltic Sea lagoons occurs almost every winter, with periods of ice coverage lasting in cold years for up to 2 months, and maximum ice thicknesses of 30 cm being reported. As late winter and early spring are also the periods when ozone depletion events have been observed in the northern hemisphere (Bojkov et al. 1995), it is particularly important to consider the spectral irradiance composition under ice.

The underwater light climate at times when the water is frozen are determined by the optical properties of both the overlying ice and the water body itself. Figure 3 shows attenuation spectra of different kinds of ice observed throughout the DZBK during the severe winter of 1996. Whereas pure ice (“clear ice”) has a rather poor spectral dependency and an attenuation of 8–9 m^{-1}, this formation of ice was rarely found. Instead, the predominant type of brackish water ice included wind-blown dust particles and small air bubbles, leading to a pronounced wavelength-dependent scattering effect and higher overall attenuation. Almost complete darkness was observed under the ice when additional snow cover was present, even if the snow layer was only a few millimetres thick as in the example presented in Fig. 3. Additionally, and despite a reduction in the particulate load, the cDOM content of the water column remained high during periods of prolonged freezing, so that the UV attenuation of the unfrozen water body was unaffected. Water column UV attenuation coefficients at 350 nm of 11 m^{-1} for Bodstedter Bodden, and 7.5 m^{-1} for Grabow were measured (Fig. 3), both falling within the range of K_d values measured at other times of year.

The data presented so far enable the spectral composition and intensity of irradiance for any given depth and location within the estuary to be calculated, given accurate knowledge of the irradiance immediately below the surface, and the concentrations of cDOM and chlorophyll *a*. However, for phytoplankton as well as for benthic algae, there are several additional factors which affect the relationship between the above-surface and subsurface irradiances. These will be discussed in the following section.

Variations of subsurface irradiance due to changes in solar elevation and atmospheric conditions

The effect of variation in solar elevation on the availability of light at the earth’s surface is almost fully understood (Michalsky 1988; Spencer 1989), and can be handled by numerical analysis (Walsby 1997). However, surface irradiance is only in part dependent on the solar elevation but also greatly influenced by weather conditions, especially cloud cover and transparency of the atmosphere. The quantity and spectral composition of surface UV-B is additionally dependent upon the ozone concentration of the upper atmosphere, which can change on a time scale of days.

A comparison between a yearly set of PAR and UV-B measurements at the investigation area with the calculated maximum daily doses showed considerable deviation between the predicted and the measured values (Fig. 4). The measured daily doses rarely reached the theoretical maximum values. Moreover, because of the pronounced seasonal weather patterns, the extent of the deviations from the maximum daily doses differed throughout the year.

The variations in maximum daily dose shown in Fig. 4 are the result of two effects: first the changes in maximum zenith angle and second the seasonal changes in daylength. For the aquatic environment an additional amount of irradiance will be lost due to reflection at the water/air boundary, and this loss increases at lower solar angles.

We measured the reflective loss at the air/water boundary as solar elevation changed (Fig. 5), and found a substantial deviation from the values predicted by Snel's law of reflection. A maximum reflection of only 30% occurred, in contrast to the total reflection which was to be expected at very low solar angles. Therefore the reduction of daylength in the aquatic environment because of solar angle dependency of reflection seems questionable. The reason for this deviation from Snel's law, already recognised and discussed by e.g. Dekker (1993) or Austin (1974) is rather simple. We made measurements during a typical weather situation with wind speeds around 4 m s^{-1}, and the water surface was roughened by waves and not mirror flat. The effect caused by wind roughening is illustrated in Fig. 6. The lower part of the left-hand photo of Fig. 6 depicts a situation with a flat calm surface, in this case reflection occurs at the reverse angle to the incident solar elevation, and is maximal. In the right-hand part of Fig. 6 the water surface is disturbed and a reflection continuum is visible. Total reflection was considerably lower. Reflection is dependent on the form of the water surface, which is normally made uneven by waves. At low solar angles, photons are only reflected on the narrow crests of the waves, whereas photons can enter the wave fronts without significant reflection. The back surface of the waves, on the other hand, do not receive direct solar irradiance, but can refract light which has already entered the wave back into the water body, thus diminishing the reflective loss. A continuous recording of wind speed and surface roughness is therefore required for converting measurements of surface irradiance to sub-surface irradiance. During cloudy conditions, the calculation of reflective loss is greatly simplified, as surface irradiation is evenly distributed over most of the sky's hemisphere. A constant reflective loss of 6.6% can be assumed for a smooth water surface (Preisendorfer 1988; Dekker 1993).

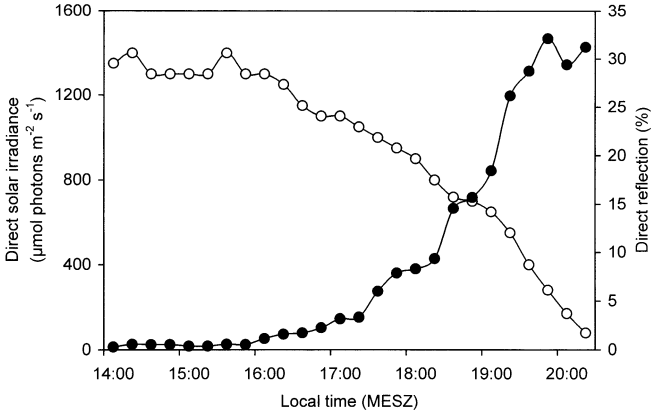

Fig. 5 Direct solar irradiance and percentage of directly reflected solar irradiance measured during a clear sky situation on the Baltic Sea at Wustrow, in June 1994. Measurements were done with a cosine-corrected PAR sensor shielded with a black tube of 10 cm length to give an acceptance angle of 17°. The sensor was directed at the sun (to measure direct solar irradiance, *open circles*) or at the sun's reflection on the sea surface (to measure direct reflection, *filled circles*)

Fig. 6 Reflection at low solar elevation at an disturbed (*lower part of the right-hand photo* and *middle parts of both photos*) and an undisturbed (*lower part of the left-hand photo*) water surface

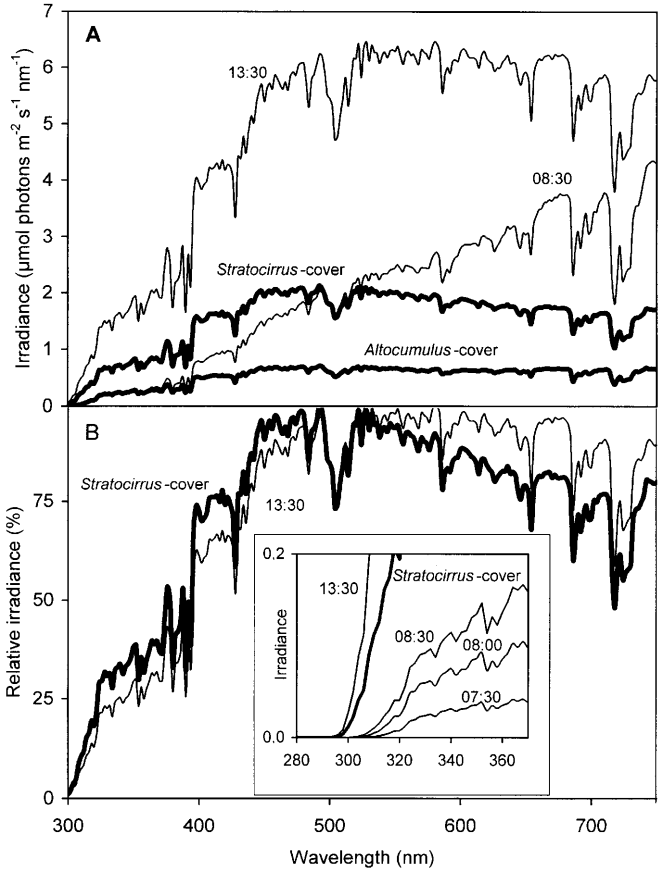

Fig. 7 Spectral composition of surface irradiance during different weather conditions and solar elevations. Surface spectra were measured on 14 September 1999 during a clear sky situation (*upper panel*, *solid lines*) at solar elevations of 8° (0730 hours MESZ), 12° (0800 hours MESZ), 17° (0830 hours MESZ) and 41° (1330 hours MESZ). As a comparison, spectra recorded underneath 8/8 *Stratocirrus* cover (*upper thick line*, 39° solar elevation, 30 August 1999, 1300 hours MESZ) and 8/8 *Altocumulus* cover (*lower thick line*, 38° solar elevation, 19 August 1999, 1335 hours MESZ) are included. The *lower panel* shows the 1330 hours (*thin line*) and *Stratocirrus* (*thick line*) spectra normalised to 1 at their maximum values. The *inset* shows the elevation and cloud cover dependency of irradiance (µmol photons m^{-2} s^{-1} nm^{-1}) of the UV region on expanded scales

Differences in solar elevation and weather conditions also cause variability in the spectral composition of surface irradiance. The extent to which the changing solar elevation can change the spectral composition over the course of a clear summer day is shown in Fig. 7a. The shorter wavelengths of UV and blue light are deficient during early morning and late evening, due to the increased pathlength through the atmosphere and greater molecular scattering. As a consequence, the shortest wavelengths of UV-B are concentrated in a relatively short period around solar noon (Fig. 7b inset). The spectral shifts caused by cloud cover are not so pronounced as those caused by changes in the elevation of the sun. At midday, increasing cloud cover causes a slight shift in the spectrum towards shorter wavelengths, as the influence of the direct solar beam is then less important (Fig. 7b).

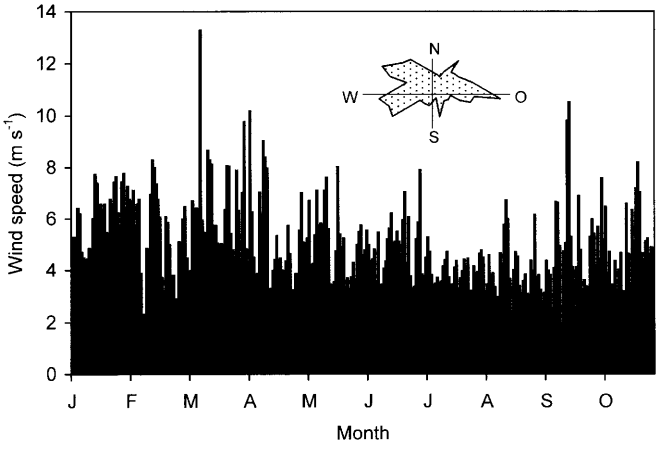

Fig. 8 Wind speed and wind direction measured at Zingst during 1994. The graph shows daily averages of wind speed (*main graph*) and wind direction (*inset*) measured at the station Zingst, located directly beside the mid-point of the estuary

The accuracy of modelling the mean spectral irradiance distribution at any position in the water column will be increased with parameterisation of both topics presented above. In the following section the high frequency variations which are superimposed on this mean light availability will be presented.

Variations of subsurface irradiance due to Langmuir circulation and wave focussing

Despite the fact that the wind-driven vertical circulation of the upper water layer, the so called “Langmuir circulation”, has long been known, and can be easily detected at higher wind speeds by the characteristic parallel foam bands, only a few direct measurements of the kinetics of circulation have been published (e.g. Denman and Gargett 1983, 1995). The reason for the lack of quantitative information is that this type of circulation, often simplified as circle-like, is rather complex, consisting of a mixture of several spiral-like eddies rotating at speeds in the centimetre per second range. Tracer materials are diluted and drift horizontally, so that it is hard to obtain reliable field measurements of wind-driven circulation. However, careful use of fluorescent dyes can permit water-circulation time to be measured, and high-resolution temperature profiling can be used to measure mixing depth (MacIntyre 1993). In the Darss-Zingst estuary, no temperature gradient could be detected at two shallow investigation sites (0.8 and 1.5 m). It was concluded that the water column was mixed to the bottom. At both sites, measurable vertical movement could be detected from wind speeds starting at 2 m s^{-1}, a value which fits quite well to the observations published by e.g. Horne and Wrigley (1975). A higher value of 2–3 m s^{-1} for the onset of vertical mixing for surface scums of gas-vacuolate cyanobacteria was published by Webster and Hutchinson (1994) and Hutchinson and Webster (1994).

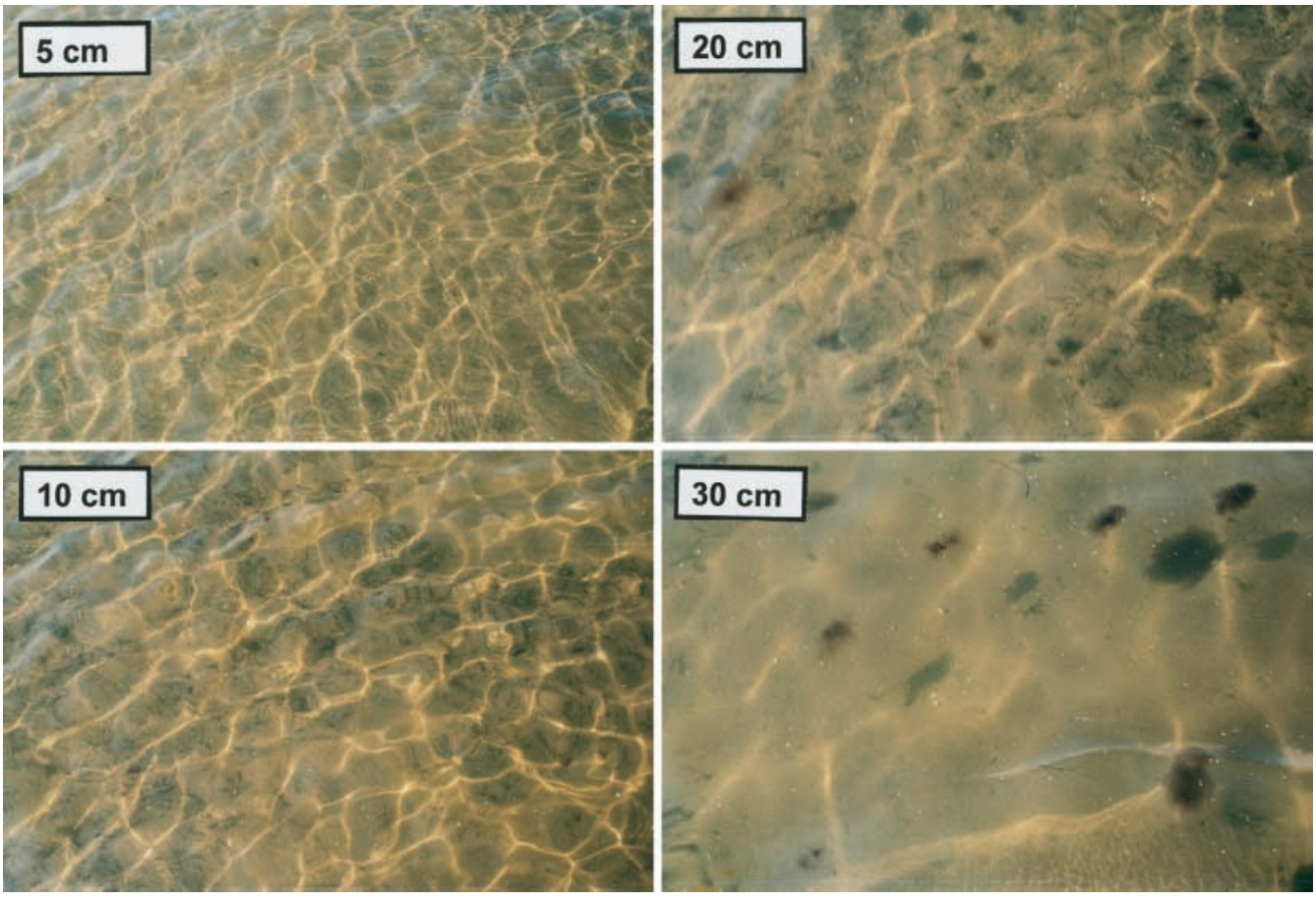

Fig. 9 Wave focussing at different water depths (*top left*, 5 cm; *bottom left*, 10 cm; *top right*, 20 cm; *bottom right*, 30 cm). The photographs were all taken at a distance of 1.8 m above ground, so distance between the individual focussing lines represents their frequency as well

It can be assumed that complete mixing of the whole water column of the shallow areas of the Darss-Zingst estuary will occur at windspeeds of approximately 2 m s^{-1} and above. This assumption matches well to observations that, excluding periods of ice cover, almost no vertical temperature gradients could be measured in the system (Schubert et al. 1997). An exception was sometimes to be observed in the outermost part of the bodden chain, the Grabow, in which sudden inflows of colder, salt-rich water occasionally lead to a temporary stratification of the water column.

Wind speed measurements taken at the investigation site during 1994 showed that the wind speed almost always exceeded the minimum for onset of mixing (Fig. 8). The main axis of the estuary is located in a west-east direction, which closely matches the prevailing wind direction (Fig. 8), so the contact between wind and water, which is necessary to drive mixing, is large. On only 4% of days was the minimum wind speed necessary for complete vertical mixing not achieved. This infrequent occurrence of calm days was due to the location of the sampling site on the Baltic Sea coast. Here, even under anticyclonic conditions when pressure-driven wind speeds were low, differential heating of land and sea caused a typical regime of onshore and offshore breezes to be established.

The time needed for a particle to complete one full Langmuir circulation in a 2-m-deep water column was estimated as approximately 20 min (Schubert and Forster 1997). During the circulation an irradiance gradient is traversed which ranges from high irradiance, full spectral exposure near the surface, down to <1% at the bottom, and back to 100%. This circulation exposes phytoplankton to variations in the PAR and UV-radiation regime which are considerably faster than the reaction times of biochemically based acclimation strategies.

However, even faster changes in irradiance occur near the surface. Waves act as lenses because of the differences in refractive indices between air and water, and light is focussed below the wave for a brief period. In shallow water, this effect can be seen clearly by eye (Fig. 9), appearing against a dark background as flickering bands of focussed light. It can also be seen from the sequence of photographs of different depths that the intensity and frequency of the focussing events are reduced as water depth increases. The location of the focussing events depends upon the shape of the waves. Large, rounded waves focus into deeper regions than small, sharply curved ripple waves.

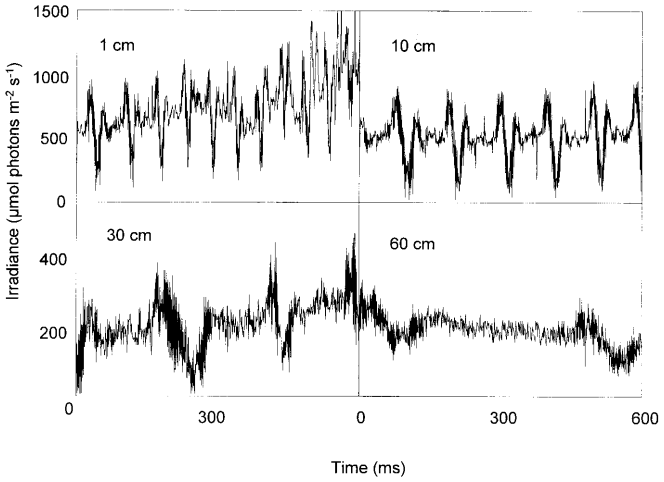

Fig. 10 Wave-focussing records at different depths. Individual high-frequency records of extremely short-term fluctuations of PAR, measured in the Baltic Sea during a storm event on 29 September 1995. The data were logged between 1000 and 1130 hours at a measuring frequency of 1 ms, with the presence of unbroken cloud cover (8/8 *Altostratus translucidus*). Shown are the records with maximum amplitudes of PAR fluctuations (compare also with Fig. 11 *main graph*)

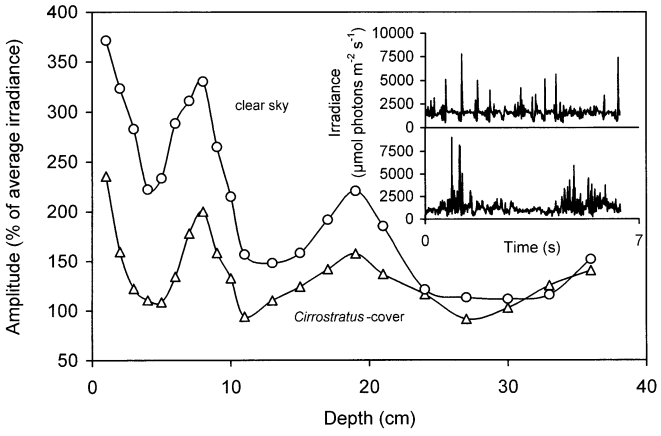

Fig. 11 Depth profile of the wave-focussing effect. Shown in the *main graph* are vertical profiles of the magnitude of the wave-focussing effect (amplitude expressed as percentage of the average irradiance) measured at Zingst during a clear sky situation (*open circles*) and underneath an 8/8 *Cirrostratus* cover (*open triangles*). The *inset* shows individual records of wave-induced short-term irradiance fluctuations, measured with a logging interval of 10 ms, at a depth of approximately 1 cm below the wave troughs for the DZBK at Zingst (*upper panel*), and for the Baltic Sea (*lower panel*), recorded at noon during a clear sky situation. The sensor was kept at a fixed position for these measurements and the record was started at the moment the wave trough passed by

An underwater irradiance detector was connected to a digital recording system with extremely fast time resolution in order to quantify wave-focussing effects. A depth series of time-resolved irradiance measurements taken with this equipment at the Baltic during a storm situation is shown in Fig. 10. Four distinct focussing levels, shown here, could be identified, differing in amplitude and frequency, which were most probably caused by the different superimposing wave types. The relatively low absolute amplitude was due to cloud cover, which was 8/8 *Altostratus translucidus* during the measurements. The inset in Fig. 11 shows as a comparison similar measurements for the uppermost focussing level made in the open Baltic and in the DZBK during clear sky conditions. Small ripple waves were present at both locations, but during the measurements in the Baltic Sea these smaller waves were accompanied by larger waves passing more slowly through the site. During the passage of a larger wave crest, the sensor was no longer located at the focussing maximum. This can be seen between 2.5 and 4 s for the Baltic time series. The wave-focussing events caused by the very small ripple waves are therefore visible only during passage of the larger wave troughs, e.g. at 1–2 s and 5–6 s in the Baltic time series. In the more sheltered DZBK location there were only ripple waves, and an almost continuous series of wave-focussed maxima at the 1-cm measuring depth was observed.

The magnitude of increased irradiance which occurred due to wave focussing was clearly evident in both sets of measurements. In both cases peaks of almost 9,000 µmol photons m^{-2} s^{-1} could be detected for short periods, which is fivefold higher than the average subsurface irradiances.

Figure 11 shows depth profiles of wave-focussing effects, where the amplitude of the wave focussing is expressed as a percentage of the mean irradiance. The wave conditions present on this day caused the appearance of three distinct wave-focussing levels, at depths of 1 cm, 8 cm and 19 cm and a possible broader focussing level at 35 cm. The decreasing amplitude with increasing depth was due to strong absorption and scattering of the estuarine water which diminish and broaden the focussed beams.

The large decrease in the absolute importance of wave focussing in cases of cloud cover can be seen by comparing the clear sky measurements with those made under thin cloud cover (Fig. 11). The *Cirrostratus* cover was completely translucent, with an average subsurface irradiance of approximately 1,700 µmol photons m^{-2} s^{-1}, but due to the absence of a direct solar beam, the amplitude of focussing events was decreased to half the values reached with clear sky.

Discussion

The attenuation spectra presented here show that the optical properties of the water bodies present along the DZBK are dominated by the exceptionally high load of phytoplankton and cDOM. Attenuation in the long-wavelength range is mainly caused by photosynthetic pigments, whereas cDOM absorption dominates in the short wavelength range, including UV. The strong attenuation results in a compression of the light gradient within a short vertical distance. Measuring attenuation values in

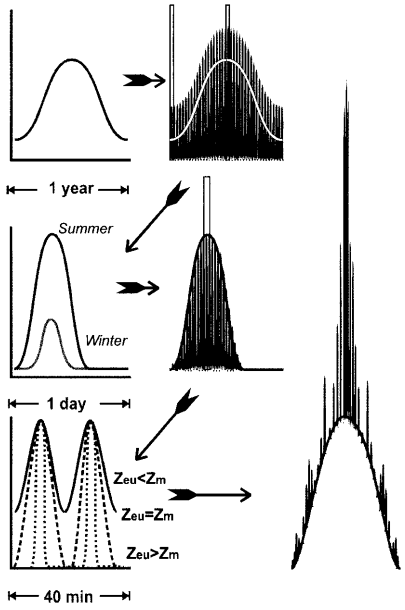

Fig. 12 Summary of the time scales of the short-, mid- and long-term levels of variability in underwater irradiance. The uppermost graph shows the annual variability in daily PAR dose (*left*), with daily fluctuations in PAR superimposed on the *right-hand graph*. The *middle section* shows on the *left-hand side* the idealised daily course of surface irradiance for days in winter and in summer, with the effect of clouds or vertical mixing shown on the *right*. The *lowermost graph* shows the changes in irradiance which could occur on a short time-scale (40 min) when an algal cell becomes entrained in a wind-mixed water body. Situations are shown in which the euphotic depth is deeper than the mixing depth ($Z_{eu}>Z_m$, *solid line*), euphotic depth is equal to the mixing depth ($Z_{eu}=Z_m$, *dashed line*), and euphotic depth is shallower than the mixing depth ($Z_{eu}<Z_m$, *dotted line*). Additionally, the algal population will be exposed to high frequency irradiance fluctuations near the surface (*furthermost right*)

waters of this type requires the use of a very small sensor with high sensitivity as well as an almost motionless water surface to enable depth measurements on a centimetre scale, prerequisites which are given by only a few instruments, and on few measuring occasions. A small sensor diameter is also important to prevent self-shading, a fact which often restricts the reliability of measurements in turbid waters.

In addition to the steep vertical gradient in light availability, a series of irradiance fluctuations occur which influence the availability of light for planktonic and benthic organisms. Solar-angle-dependent fluctuations of daily irradiance dose, as depicted in the uppermost part of Fig. 12 are slow, so that the system can react by changes in, for example, the phytoplankton succession (Schubert 1996a), or by changes in pigmentation within the population.

The predictable, seasonal fluctuations in subsurface UV-R and PAR are, of course, modified by weather conditions and, as can be seen from Fig. 3, periods of ice cover. In contrast to some other findings, e.g. those of Legendre et al. (1981), who investigated a region with predominantly clear ice, we observed in the DZBK a very turbid form of ice originating from several freeze-thaw cycles, and giving a very high attenuation. Ice cover, in combination with snow cover, resulted in almost complete darkness in the water. In addition, short-wavelength attenuation of the water body itself remained high during periods of ice cover due to a high cDOM concentration. There was no evidence of increased UV penetration immediately after ice melting which may have caused for example inhibition of phytoplankton development at the beginning of the bloom period (compare Figs. 3 and 1).

Within the course of a day, the changes in irradiance supply are dependent primarily on the solar elevation, with an additional large effect due to changing weather conditions. Both factors influence the intensity and spectral composition of irradiance at the water surface. Whereas solar-angle-dependent changes in absolute irradiance can be estimated by means of numerical models (Walsby 1997), spectral changes which depend on climatic conditions are very difficult to model in this way. The database obtained by our measurements so far does not allow the spectral composition of surface light to be constrained, for example by using the ratio of predicted irradiance to actual measured irradiance. Therefore, in the case of ecophysiological investigations dealing with effects caused by narrow parts of the solar spectrum (as with UV-B), on-site measurements are still absolutely necessary, and cannot be replaced by simulations.

Tidal movement causes an additional cause of variability in the coastal marine environment. In the case of the Baltic estuaries and lagoons, regular tides are absent, but water level fluctuations do occur irregularly, caused mainly by air pressure changes. Dring and Lüning (1994) and Sagert (1999) describe the effects of tidal movement on the underwater light climate, particularly for benthic organisms, in detail.

However, for phytoplankton and zooplankton, a more important fluctuation in irradiance exposure is caused by wind-induced vertical movement, such as the Langmuir convection (Fig. 12, lower part). In the area of our investigations, this convection was found to occur from wind speeds of greater than 2 m s^{-1}, a condition which was met on 96% of all days. The average time for one complete movement of a particle through a Langmuir spiral was 20 min, in which time a gradient of irradiance, from surface irradiance down to possibly darkness, would be encountered (Schubert and Forster 1997). Considerable differences in intensity and strong shifts in spectral composition occur during this circulation. Despite the short period of these changes, it has been shown that biophysical changes in phytoplankton physiology can be induced (Schubert et al. 1995a). Phytoplankton have also been shown to react to simulated vertical mixing as opposed to continuous light with alterations in their photosynthetic parameters (Kroon et al. 1992; Ibelings 1992; Schubert et al. 1995b).

The final level of irradiance variability, with the highest frequency, is wave focussing, which occurs in addition to

all of the other mechanisms listed above (Fig. 12, bottom right). An analogous situation occurs in the understorey regions of terrestrial forests, where movement of the canopy allows short bursts of sunlight to reach the lower vegetation. Wave focussing is however more intense, causing an amplification of irradiance of up to 5 times the mean subsurface intensity, and the events last for very short periods of time (millisecond range). This range of values matches that predicted and measured in laboratory systems by Stramski and Legendre (1992). The absolute irradiance measured at the focussing depth was found to depend on the amount of light captured by the wave, and thus its area. The size and intensity of the focussed light spot were also influenced, in our case heavily, by the attenuation characteristics of the water body, and wave focussing was most prominent under clear sky conditions. The rate of occurrence of individual focussing events at a certain depth depended entirely on the frequency of the passing waves.

There is at present little known about the physiological effects caused by prolonged exposure to these short, supersaturating flashes of PAR and UV-R. All investigations performed so far in the laboratory have been done by applying a constant flash regime, which will, because of vertical movement, never be present in the field. More detailed studies of the physiological effects of wave focussing, as well as detailed analyses of the theoretical background, have been restricted to macrophytic algae (Wing and Patterson 1993; Kübler and Raven 1996), so more knowledge is needed to decide whether or not deleterious effects on phytoplankton must be expected.

Acknowledgement This work was supported by a grant of the German Ministry of Education and Research (BMBF, grant no. BEO/52/F0266D), which is gratefully acknowledged. The experiments performed complied with the current laws of the country in which they were performed.

References

Allen JF (1992) Protein phosphorylation in regulation of photosynthesis. Biochim Biophys Acta 1098:55–335

Austin RW (1974) The remote sensing of spectral radiance from below the ocean surface. In: Jerlov NG, Steeman Nielsen E (eds) Optical aspects of oceanography. Academic Press, London, pp 316–344

Barber J, Andersson B (1992) Too much of a good thing: light can be bad for photosynthesis. Trends Biochem Sci 17:61–66

Björn LO, Murphy TM (1985) Computer calculation of solar ultraviolet radiation at ground level. Physiol Veg 23:555–561

Bojkov, RD, Fioletov VE, Balis DS, Zerefos CS, Kadygrova TV, Shalamjansky AM (1995). Further ozone decline during the northern-hemisphere winter–spring of 1994–1995 and the new record low ozone over Siberia. Geophys Res Lett 22: 2729–2732

Bornitz R, Gagelmann J (1995) Entwicklung und Erprobung eines Programmpaketes zur Datenerfassung und Visualisierung für das Meßsystem zur Unterwasser-Lichtmessung. Belegarbeit, Universität Rostock, Rostock

Dekker AG (1993) Detection of optical water quality parameters for eutrophic waters by high resolution remote sensing. Thesis. Vrij Universiteit Amsterdam, Amsterdam

Denman KL, Gargett AE (1983) Time and space scales of vertical mixing and advection of phytoplankton in the upper ocean. Limnol Oceanogr 28:801–815

Denman KL, Gargett AE (1995) Biological physical interactions in the upper ocean – the role of vertical and small-scale transport processes. Annu Rev Fluid Mech 27:225–255

Dring MJ, Lüning K (1994) Influence of spring-neap tidal cycles on the light available for photosynthesis by benthic marine plants. Mar Ecol Prog Ser 104:131–137

Falkowski PG, LaRoche J (1991) Acclimation to spectral irradiance in algae. J Phycol 27:8–14

Franklin LA, Forster RM (1997) The changing irradiance environment consequences for marine macrophyte physiology, productivity and ecology. Eur J Phycol 32:207–32

Horne AJ, Wrigley RC (1975) The use of remote sensing to detect how wind influences planktonic blue-green algal distribution. Int Ver Theor Angew Limnol Verh 19:784–791

Hutchinson PA, Webster IT (1994) On the distribution of blue-green algae in lakes: wind-tunnel tank experiments. Limnol Oceanogr 39(2):374–382

Ibelings BW (1992) Cyanobacterial waterblooms: the role of buoyancy in watercolumns of varying stability. Thesis. Universiteit van Amsterdam, Amsterdam

Jerlov NG (1951) Optical studies of ocean water. Rep Swed Deep-Sea Exped 3:1–59

Jerlov NG (1976) Marine optics. Elsevier, Amsterdam

Kirk JTO (1994) Light and photosynthesis in aquatic ecosystems. Cambridge University Press, Cambridge

Kromkamp J, Schanz F, Rijkeboer M, Berdalet E, Kim B, Gons HJ (1992) Influence of the mixing regime on algal photosynthetic performance in laboratory scale enclosures. Hydrobiologia 238:111–118

Kroon BMA, Burger-Wiersma T, Visser PM, Mur LR (1992) The effect of dynamic light regimes on *Chlorella*. Minimum quantum requirement and photosynthesis-irradiance parameters. Hydrobiologia 238:79–89

Kübler JE, Raven JA (1996) Nonequilibrium rates of photosynthesis and respiration under dynamic light supply. J Phycol 32: 963–969

Legendre L, Ingram RG, Poulin M (1981) Physical control of phytoplankton production under sea ice (Manitounuk Sound, Hudson Bay). Can J Fish Aquat Sci 38:1385–1392

MacIntyre S (1993) Vertical mixing in a shallow, eutrophic lake: Possible consequences for the light climate of phytoplankton. Limnol Oceanogr 38:798–817

Michalsky JJ (1988) The Astronomical almanac's algorithm for approximate solar position (1950–2050). Solar Energy 41: 227–235

Piazena H, Häder D-P (1994) Penetration of solar uv irradiation in coastal lagoons of the southern baltic sea and its effect on phytoplankton communities. Photochem Photobiol 60: 463–469

Porra RJ, Thompson WA, Kriedemann PE (1989) Determination of accurate extinction coefficients and simultaneous equations for assaying chlorophylls *a* and *b* extracted with four different solvents: verification of the concentration of chlorophyll standards by atomic absorption spectroscopy. Biochim Biophys Acta 975:384–394

Preisendorfer RW (1988) Principal component analysis in meteorology and oceanography. Elsevier, New York

Sagert S (1999) Ökophysiologische Untersuchungen an Rhodophyceen: Vergleichende Studien zum Faktor Licht. Thesis. Univeristy of Rostock, Rostock

Schiewer U, Schlungbaum G, Arndt EA (1993) Monographie der Darss-Zingster Boddenkette. Rostock Meeresbiol Beitr 2: 240 pp

Schubert H (1996a) Starklichtanpassungs-Strategien von Grünalgen und Cyanobakterien. Nova Acta Leopold Suppl 14: 109–124

Schubert H (1996b) Ökophysiologie der Lichtanpassung des Phytoplanktons eutropher Flachgewässer. Thesis. University of Rostock, Rostock

Schubert H, Forster RM (1997) Sources of variability in the factors used for modelling primary productivity in eutrophic waters. Hydrobiologia 349:75–85

Schubert H, Forster RM, Sagert S (1995a) In situ measurement of state transition in cyanobacterial blooms – kinetics and extent of the state change in relation to underwater light and vertical mixing. Mar Ecol Prog Ser 128:99–108

Schubert H, Matthijs HCP, Mur RL, Schiewer U (1995b) Blooming of cyanobacteria in turbulent water with steep light gradients: the effect of intermittent light and dark periods on the oxygen evolution capacity of *Synechocystis* sp. PCC 6803. FEMS Microbiol Ecol 18:237–245

Schubert H, Forster RM, Schoor A, Ockenfeld K (1997) Horizontale und vertikale Chlorophyllverteilung des Bodstedter Boddens. Rostock Meeresbiol Beitr 5:69–84

Smith RC (1968) The optical characterisation of natural waters by means of an extinction coefficient. Limnol Oceanogr 13:423–429

Smith RC, Baker KS (1981) Optical properties of the clearest natural waters. Appl Optics 20:177–184

Spencer JW (1989) Comments on the astronomical almanac's algorithm for approximate solar position (1950–2050). Solar Energy 42:353

Stramski D, Legendre L (1992) Laboratory simulation of light-focusing by water-surface waves. Mar Biol 114:341–348

Stramski D, Rosenberg G, Legendre L (1993) Photosynthetic and optical properties of the marine chlorophyte *Dunaliella tertiolecta* grown under fluctuating light caused by surface-wave focusing. Mar Biol 115:363–372

Tichy V, Poulson M, Grobbelaar JU, Xiong F, Nedbal L (1995) Photosynthesis, growth and photoinhibition of microalgae exposed to intermittent light. In: Mathis P (ed) Photosynthesis: from light to biosphere, vol V. Kluwer, Dordrecht, pp 1029–1032

Trenkensu AP, Beljanin VN, Sidko FJ (1976) Photobiosynthesis of the microalga *Synechococcus elongatus* upon exposure to intermittent light. Arch Hydrobiol Suppl 49 Algo Stud 15: 176–184

Walsby AE (1997) Numerical integration of phytoplankton photosynthesis through time and depth in a water column. New Phytol 136:189–209

Webster IT (1990) Effect of wind on the distribution of phytoplankton cells in lakes. Limnol Oceanogr 35:989–1001

Webster IT, Hutchinson PA (1994) Effect of wind on the distribution of phytoplankton cells in lakes revisited. Limnol Oceanogr 39(2):365–373

Wing SR, Patterson MR (1993) Effects of wave-induced light-flecks in the intertidal zone on photosynthesis in the macroalgae *Postelsia palmaeformis* and *Hedophyllum sessile* (Phaeophyceae). Mar Biol 116:519–25

Wing SR, Leichter JJ, Denny MW (1993) A dynamic model for wave-induced light fluctuations in a kelp forest. Limnol Oceanogr 38:396–407